energies

MDPI

Article

Model of Flow Resistance Coefficient for a Fragment of a Porous Material Deposit with Skeletal Structure

Grzegorz Wałowski [1,2]

[1] Institute of Technology and Life Sciences—National Research Institute, Falenty, Al. Hrabska 3, 05-090 Raszyn, Poland; g.walowski@itp.edu.pl
[2] Department of Renewable Energy, 67 Biskupinska Street, 60-463 Poznan, Poland

Abstract: The hydrodynamic conditions resulting from the permeability of porous materials are based not only on the assessment of the gas flow through these materials, but also the losses related to the pressure energy in this flow. Flow resistance is a direct measure of this loss. The aim of this experimental research was to evaluate the flow resistance of the porous material in relation to the gas flow. The research was carried out on a material with a slit-porous structure. The tests were carried out on a system for measuring gas permeability under the conditions of gas bubbling through the char. The issue of the total pressure drop process in the porous bed was considered in the Reynolds number category. The coefficient of flow resistance for the char was determined and the value of this coefficient was compared with the gas stream, and an experimental evaluation of the total pressure drop on the porous bed was made. The novelty of this article is the determination of the tortuosity and the gas permeability coefficient for a solid of any shape—a rigid skeleton.

Keywords: flow resistance; gas; porous material; permeability

Citation: Wałowski, G. Model of Flow Resistance Coefficient for a Fragment of a Porous Material Deposit with Skeletal Structure. *Energies* **2021**, *14*, 3355. https://doi.org/10.3390/en14113355

Academic Editor: Robert Castilla

Received: 25 April 2021
Accepted: 3 June 2021
Published: 7 June 2021

1. Introduction

Under natural conditions, the flow of fluids in porous structures is connected with the movement of gases and liquids in geological deposits [1]. These deposits, as primary reservoirs, are areas of migration [2–15] of such substances as crude oil or natural gas, but also of the movement of other liquids and gases, such as water brine or methane in rock masses of hard coal. In each of these cases, recognizing conditions of the flow of gasses by porous deposits can, to a considerable degree, contribute to better understanding mechanisms of the flow and the migration of gasses in the given rock deposit, which can also correlate with more effectively getting gas out of natural geological deposits. This is all the more important as the growing industrialization causes the economy to become increasingly interested in additional energy resources.

Hydrodynamic conditions resulting from the permeability of porous materials have their base not only in the evaluation of the stream of the flow of gas through such materials but also losses concerning the pressure energy in this flow. The direct measure of that loss is flow resistance, which may be interpreted differently in the detailed quantitative assessment. By analyzing research studies [16–23] on modelling resistances of the flow through porous deposits, it can be noticed that the authors consider the movement criterion of the Reynolds number [16,24] and interpret hydrodynamic conditions of that flow in a different manner. On the other hand, modifications to the Darcy–Weisbach [22,23] Equation (1) that enables calculating the flow resistances most frequently refer to granular structures or porous deposits in the form of the permanent infill of column apparatuses.

$$\Delta P = aRe^{n-2}\frac{\rho w_e^2}{2}\frac{L}{d_e} \quad (1)$$

In which the coefficient of resistance (2):

$$\lambda_e = f(Re) = aRe^{n-2} \quad (2)$$

where the Raynolds number (3) equals to:

$$Re = \frac{w_e d_e \rho}{\eta} \quad (3)$$

However, there is no specific reference to this problem for porous materials with a solid framework structure. Assume that the coefficient of resistances defined by the Equation (4) may be representative for all those cases as an equivalent measure of flow hydrodynamics:

$$\xi = \frac{2}{\rho w^2}\Delta P \quad (4)$$

Some of those modifications were compared to the obtained measurement results. This comparison was based on the definitions of the coefficient of resistances set forth in Table 1.

Table 1. Correlation equations for calculation of a coefficient of flow resistances through granular porous structures [own elaboration].

Autor	Model Equation		Criteria Number	
Ergun [19]	$\zeta_E = \frac{150}{Re_\varepsilon} + 1.75$	(5)	$Re_\varepsilon = \frac{w_o d_\varepsilon \rho}{(1-\varepsilon)\eta}$	(6)
Brauer [25]	$\zeta_B = \frac{160}{Re_\varepsilon} + \frac{3.1}{Re_\varepsilon^{0.1}}$	(7)		
Tallmadge [26]	$\zeta_T = \frac{150}{Re_\varepsilon} + \frac{4.2}{Re_\varepsilon^{0.1666}}$	(8)		
Burke-Plummer [27]	$\zeta_{B-P} = 0.878\frac{(1-\varepsilon)}{\varepsilon^2}$	(9)		
Blake-Kozeny [27]	$\zeta_{B-K} = 75\frac{(1-\varepsilon)^2}{\varepsilon^3}\frac{1}{Re_\varepsilon}$	(10)	$Re_\varepsilon = \frac{w_o d_\varepsilon \rho}{\eta}$	(11)
Blake-Kozeny-Carman [20]	$\zeta_{B-K-C} = \frac{180}{Re_\varepsilon}$	(12)		
Żaworonkow [28]	$\zeta_Z = \frac{3.8}{Re_\varepsilon^{0.2}}$	(13)	$Re_\varepsilon = \frac{w_o d_\varepsilon \rho}{\varepsilon\eta}$	(14)
Windsperger [29]	$\zeta_W = 2.2\left(\frac{0.4}{\varepsilon}\right)^{0.78}\left(\frac{64}{Re_\varepsilon} + \frac{1.8}{Re_\varepsilon^{0.1}}\right)$	(15)	$Re_\varepsilon = \frac{2}{3}\frac{w_o d_\varepsilon \rho}{(1-\varepsilon)\eta}$	(16)

The values of the coefficient of resistances correspond to the resistance coefficients correlated to the models detailed in this Table at a constant quotient value of linear reference dimensions (17) [23]:

$$\frac{L}{d_\varepsilon} = 1 \quad (17)$$

The reason for this state of affairs should be seen as the high complexity of hydrodynamic phenomena for gas flow through porous materials of skeletal structure, as well as the limited possibility of adaptation of models and calculation methods characteristic of the hydrodynamics of fluid flow in closed systems.

One of those possibilities is to include in the hydrodynamics description the conditions resulting from the energy dissipation that occurs during the movement of gas in

porous and capillar spaces of porous materials. From an experimental viewpoint, this phenomenon may be associated with a certain alternative (equivalent) coefficient of resistance that include conditions resulting from the coefficient of friction between liquid and walls of flow channels and from the pressure reduction caused by the disturbance to the velocity profile characteristic for stream choking. In such a presented issue, the total resistance of gas flow through the porous deposit may be identified with the general dependency (18), considering the relevant adjustment of flow parameters of the porous structure:

$$\Delta P = \xi \frac{\rho w^2}{2} \tag{18}$$

This approach is justified by the fact that in the structure of flow micro-channels the share of friction in the flow resistance is marginal.

When directly using the Weisbach [23] Equation (18), it needs to be directly adapted to the porous structure, for which this equation may be as follows (19):

$$\Delta P = \xi_\varepsilon \frac{\rho_g w_\varepsilon^2}{2} \tag{19}$$

In this case, the flow velocity w_ε (20) refers to the section resulting from the average area of the deposit A_ε open for this flow and resulting from the porosity of the deposit ε and its complete section A_o. Hence

$$w_\varepsilon = \frac{Q_g}{A_\varepsilon} = \frac{Q_g}{\varepsilon A_o} \tag{20}$$

For such interpreted conditions, Equation (19) can be used to determine by experiment the value of the flow resistance coefficient as the value of ξ_ε, (21) which sums up all mechanisms resulting from the hydrodynamics of gas movement through porous materials:

$$\xi_\varepsilon = \frac{2}{\rho_g w_\varepsilon^2} \Delta P_{zm} \tag{21}$$

This paper attempts to describe some of the issues arising from the hydrodynamics of gas flow through a fragment of a bed under gas bubbling conditions. The proprietary model for total resistance of gas flow through a porous medium is proposed, which takes into account the bedding parameter related to the gas-permeability coefficient and porosity.

The assessment of both the stream of the gas flow through porous materials and the loss of pressure energy in that flow is an important issue not only under natural conditions, but also in practical applications. An example could be a filter used to remove particulate matter (which is mostly made of soot) from diesel engine exhaust via filtration and regeneration [30]. Another area of application of porous structural materials is the reaction process of catalytic afterburning carried out in structural reactors [31,32]. Most often, these reactors are identified with a group of monolithic reactors (so-called catalysts), equipped with ceramic cartridges with a multi-channel structure.

In particular, at the present stage of research, the permeability of char from the experimental georeactor from the Experimental Mine Barbara in Mikołów [33,34] was recognized.

The sample of the carbonate was examined by observing it under bubbling conditions. The bubbling technique was used to assess the aeration area for the porous material.

2. Materials and Methods

The research material was a solid skeleton structure derived from the technology of thermal coal gasification. Char in situ is a direct product of underground coal gasification, and it was obtained from the experimental georeactor (semi-technical scale) of the "Barbara" Experimental Mine in Poland. In this case, the process conditions favored practically complete gasification of coal, although the structure of this product is also very diverse, which, apart from the process conditions, depends on the place where the samples were obtained in the georeactor.

In quantitative terms, the following parameters were evaluated: porosity, porosity index, density (Table 2), permeability as a measure of pressure drop, and surrogate flow resistance coefficient. Irrespective of the measurement of the aeration flow, the permeability and surrogate coefficient of flow resistance were determined based on the pressure drop across the bed of the porous material. Parameters determined for studied materials (samples) are presented in Table 2.

Table 2. Characteristics of the research material [own elaboration].

Research Material (the Marking and the Source Origin of the Raw Material)		Porosity		Indicator Porosity	Density of a Solid Body	
		Absolute	Effective		Apparent	Skeleton
Name	No. Sample	ε_b, %	ε_{ef}, %	e	ϑ_a, kg/m^3	ϑ_s, kg/m^3
1	2	3	4	5	6	7
char (carbonizer)	I-1	42.2	21.1–33.7	0.7	1300	2250

2.1. Research Position

The tests were carried out on a laboratory stand. In Figure 1, the important element of which was a vessel used to assess the gas permeability phenomenon through the carbonized porous material. In Figure 2, the stand was equipped with a rotameter for measuring the gas stream and a pressure gauge. The reference pressure associated with the aeration process was determined by a reducer in the range of 0.1–0.4 MPa.

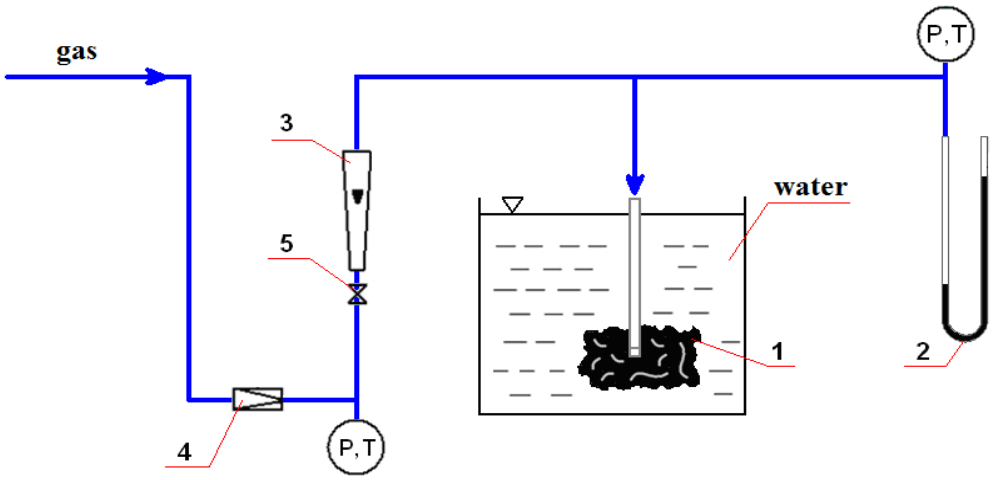

Figure 1. Diagram of the measuring system for testing the permeability of porous material in bubbling conditions [own elaboration]: 1—porous material (sample), 2—manometer of the pressure difference, 3—rotameter (3 and bubble flowmeter), 4—reducers of the pressure, 5—control valve, P—pressure indicator, T—thermometer.

Figure 2. Flow of gas in bubbling conditions—char (I-1) [Photo by Grzegorz Wałowski].

Figure 2 shows the applied system of powering the sample for the free flow of gas (with emphasizing agreed parameters) and illustrates the flow of gas in these conditions.

The shape of the sample of this type, along with the visible additive tube (are panting), are showed in Figure3 —the image refer to the volume sample char (indefinable shape). The connection of the nozzle with the porous material was made by means of a hole, and then a special adhesive (binder) was used (Figure 3).

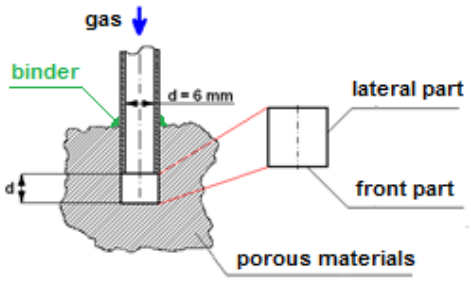

Figure 3. Supply system of volume sample [own elaboration].

In order to achieve the purpose of this research, detailed experimental tests concerning the evaluation of the permeability of gas were conducted in the structure of porous material, and the findings are presented in Table 3.

Table 3. Test results in conditions: air, 21.7 °C [own elaboration].

Research Material: Char No. Sample: I-1							
No.	***Reference Pressure P_{re}, MPa***	***Gas Stream $Q_g \cdot 10^3$, m^3/s***	***Resistance Flow Measured ΔP_{zm}, kPa***	**No.**	***Reference Pressure P_{re}, MPa***	***Gas Stream $Q_g \cdot 10^3$, m^3/s***	***Resistance Flow Measured ΔP_{zm}, kPa***
1	0.1	0.161	10.2	26	0.3	0.161	9.7
2	0.1	0.182	11.3	27	0.3	0.182	11.3
3	0.1	0.196	12.9	28	0.3	0.217	16.6
4	0.1	0.203	13.8	29	0.3	0.238	20.4
5	0.1	0.217	16.6	30	0.3	0.259	23.9
6	0.1	0.231	17.9	31	0.3	0.287	29.3
7	0.1	0.238	20.6	32	0.3	0.315	33.5
8	0.1	0.266	23.9	33	0.3	0.350	44.1
9	0.1	0.280	27.2	34	0.3	0.371	51.2
10	0.1	0.301	29.9	35	0.3	-	-
11	0.1	0.329	37.9	36	0.3	-	-
12	0.1	0.350	42.8	37	0.3	-	-
13	0.1	0.371	49.2	38	0.3	-	-
14	0.2	0.161	9.9	39	0.4	0.161	10.6
15	0.2	0.189	12.6	40	0.4	0.196	12.7
16	0.2	0.210	15.2	41	0.4	0.231	19.2
17	0.2	0.231	19.2	42	0.4	0.266	24.2
18	0.2	0.252	23.2	43	0.4	0.301	31.2
19	0.2	0.280	26.9	44	0.4	0.336	39.9
20	0.2	0.301	31.2	45	0.4	0.350	43.6
21	0.2	0.322	36.1	46	0.4	0.371	51.2
22	0.2	0.336	38.9	47	0.4	-	-
23	0.2	0.343	42.8	48	0.4	-	-
24	0.2	0.371	49.4	49	0.4	-	-
25	0.2	0.392	53.4	50	0.4	-	-

2.2. Scope and Research Methodology

The aim of the study was to evaluate the hydrodynamics of gas flow through porous materials of irregular shape. Tests were carried out using air forced through the nozzle as a stream of gas propagating in many directions in a porous bed under bubbling conditions. The gas flow resistance coefficient as a function of Reynolds number was determined. The value of the gas permeability coefficient was determined experimentally, taking into account the tortuosity. The coefficient of gas flow resistance as a function of the Reynolds number, defined for porous skeletal materials, was compared to the models known in the literature, indicating the convergence of the correlation.

3. Results and Discussion

The results for the determined flow resistance coefficient (21) for a volumetric sample are given in Figure 4.

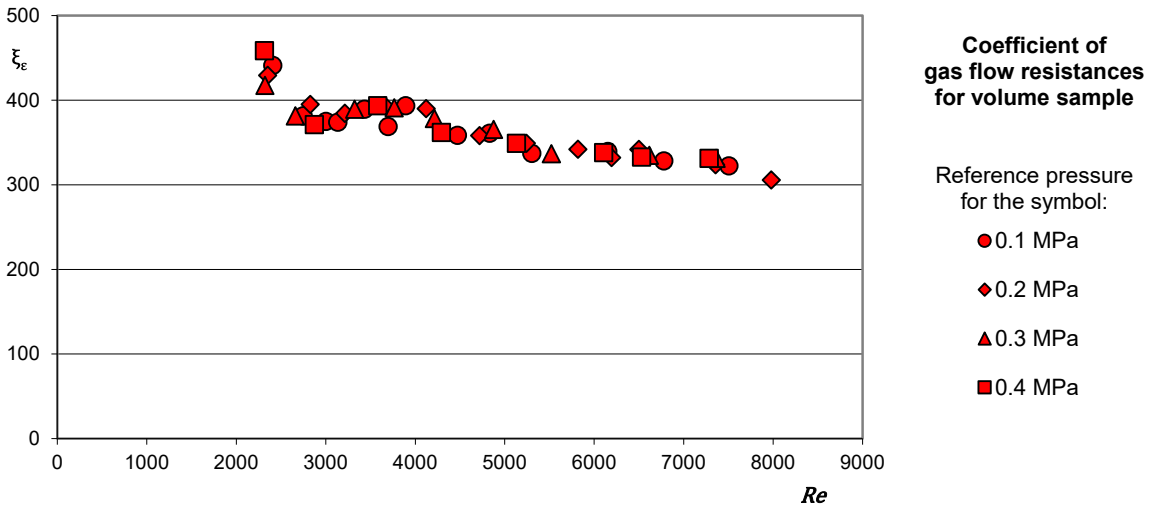

Figure 4. Coefficient of gas flow resistances for volume sample char [own elaboration].

The reference of the value of this coefficient to the Reynolds number (22) at a gas speed of w_o resulting from the d diameter of the feeding nozzle was used (Figure 3).

$$Re = \frac{w_o d \rho_g}{\eta_g} \tag{22}$$

The results show a decrease in changes to the value of the resistance coefficient as a result of an increase in the Reynolds number, which complies with the physics of the analyzed phenomena but the scale of those changes is sometimes extensive. This proves that the flow resistances are highly affected by the dynamics of gas flow through porous material, in particular by disturbances of the velocity profile. This tendency and the measuring range simultaneously indicate that for coal char (Figure 4) a turbulent nature of the gas movement is noted, which is proven by the non-linear nature of this coefficient. It may be noted that coal char has the minimum flow resistance (Figure 4). Undoubtedly, this results from the fact that this material—despite its small porosity—has a very extensive system of pores and open channels for the gas flow.

Figure 4 shows the change to the coefficient value of the resistance in proportion to the Reynolds number, and when modelling hydrodynamic conditions of the gas flow through skeletal porous material it is necessary to consider the relation (23):

$$\xi_\varepsilon = f(Re, \varepsilon) \tag{23}$$

This also refers to the Reynolds number which, in this case, may take a different form (Table 1). In the reference books, there is still a debate [35] on how to best describe this criteria number to identify the flow through frame-structured porous materials. As for those materials, it is very difficult or even impossible to assess diameters of pores and capillars and their actual flow speed. Bear and Cheng [36] suggest that in this case the Reynolds number should be defined with respect to the entire volume of the porous material referred to as the flow section.

The characteristic linear measurement is calculated as an alternative diameter resulting from the volume of the porous material and the section active for the flow, viz. (24):

$$d_{\varepsilon}^{*} = \frac{V_c}{\varepsilon A_o} \tag{24}$$

On the other hand, velocity is a result of the deposit porosity and is associated with an apparent velocity (calculated for the entire cross-section of the deposit (25)):

$$w_{\varepsilon} = \varepsilon w_o \tag{25}$$

The conducted analyses show that the method resulting from the Equations (24) and (25) and from determining the criteria Reynolds number does not reflect in the best way any hydrodynamic conditions subject to the gas flow through frame-structured porous material. This is due to the fact that the subject of the research was a sample with an irregular shape. Especially determining cross sections for the direction of flow in the case of the volume of the solid body is very difficult and imprecise. In order to solve these problems, an attempt to draw up the alternative model based on the change of characteristics of the kinetic energy for all oppositions of the flow of gas by the porous medium was made.

According to (21), this may be as follows (26):

$$\xi_{\varepsilon}(Re) = \frac{2\Delta P}{\rho_g w_{\varepsilon}^2} \tag{26}$$

Considering the diversified shape of the material and its characteristic structural features resulting from its porosity and permeability, Equation (26) may be modified by implementing a correction coefficient in the form of the so-called tortuosity parameter (27):

$$\Psi_{\varepsilon} = f(K^*, \varepsilon) \tag{27}$$

Assuming that we know the flow of gas rate, the pressure drop across the bed, and the bed porosity and the type of gas, the value of the gas permeability coefficient (28) can be determined experimentally and is defined as:

$$K^* = \frac{Q_g}{\sqrt{\frac{\Delta P_{zm}}{\rho_g}}} \tag{28}$$

Results of the measurement characteristics of a permeability coefficient of the gas of the tested sample of char are shown in Figure 5.

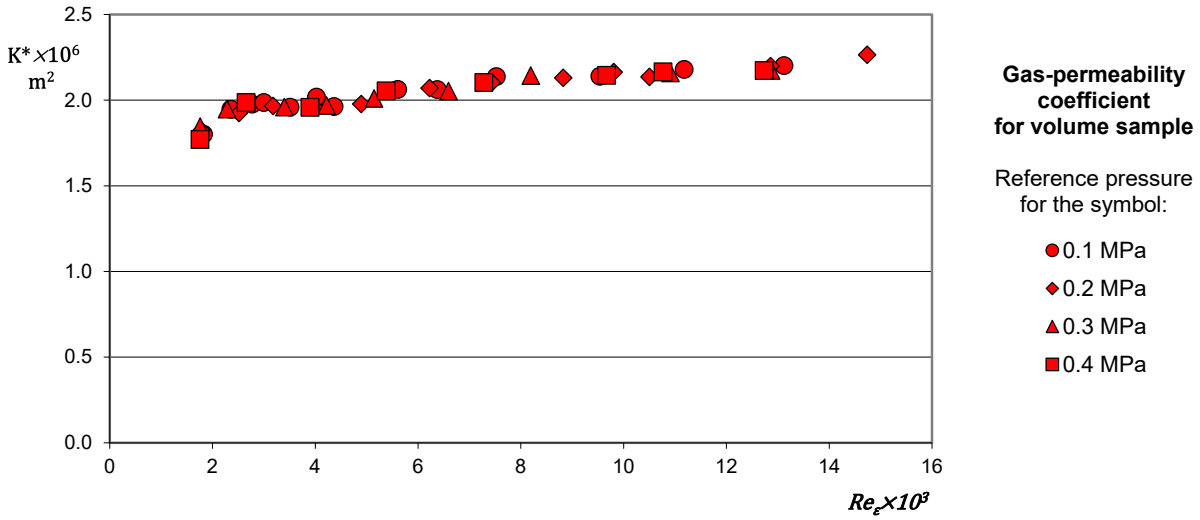

Figure 5. Gas-permeability coefficient for char [own elaboration].

The measured flow of gas flowing through the char from the total pressure drop was higher the higher the aeration pressure was, i.e., the reference pressure. On the other hand, the permeability of the char by a given value of the Reynolds number kept growing.

Taking into account dependence (27), the equation for the total coefficient of resistance is as follows (29):

$$\xi_c(Re_\varepsilon^*) = \frac{2\Delta P_c}{\rho_g w_e^2}\Psi_\varepsilon \tag{29}$$

With respect to Equation (29), the compensatory calculation was conducted for a sample in the form of an irregularly shaped solid (volume one). The arithmetical analysis shows that for the solid volume the tortuosity parameter needs to be calculated on the basis of the following dependency (30):

$$\Psi_\varepsilon = \frac{\chi_\varepsilon^a}{Re_\varepsilon^*} \tag{30}$$

The auxiliary function for the exponent a = 1.5 (char) at the base of power is the coefficient of bed formation (31) related to the gas-permeability coefficient and porosity:

$$\chi_\varepsilon = K^{*(\varepsilon-1)} \tag{31}$$

While the Reynolds number (32) takes into account the defined apparent velocity (34):

$$Re_\varepsilon^* = \frac{w_\varepsilon^* d_r \rho_g}{\eta_g} \tag{32}$$

The apparent velocity (33) refers to the entire space of the volume sample feeding as the cross-section resulting from the frontal and lateral area of the feeding nozzle Figure 3:

$$w_\varepsilon^* = \frac{Q_g}{A_o^*} \tag{33}$$

Cross-sectional area of nozzle feeding the porous material (34):

$$A_o^* = \frac{5}{4}\varepsilon_b \pi d_r^2 \quad (34)$$

The obtained results of the function of the coefficient of resistances in the function of the Reynolds number are shown in Figure 6, which, to illustrate, also include points resulting from other calculation models [19,20,25–29] adjusted by the parameters resulting from the research.

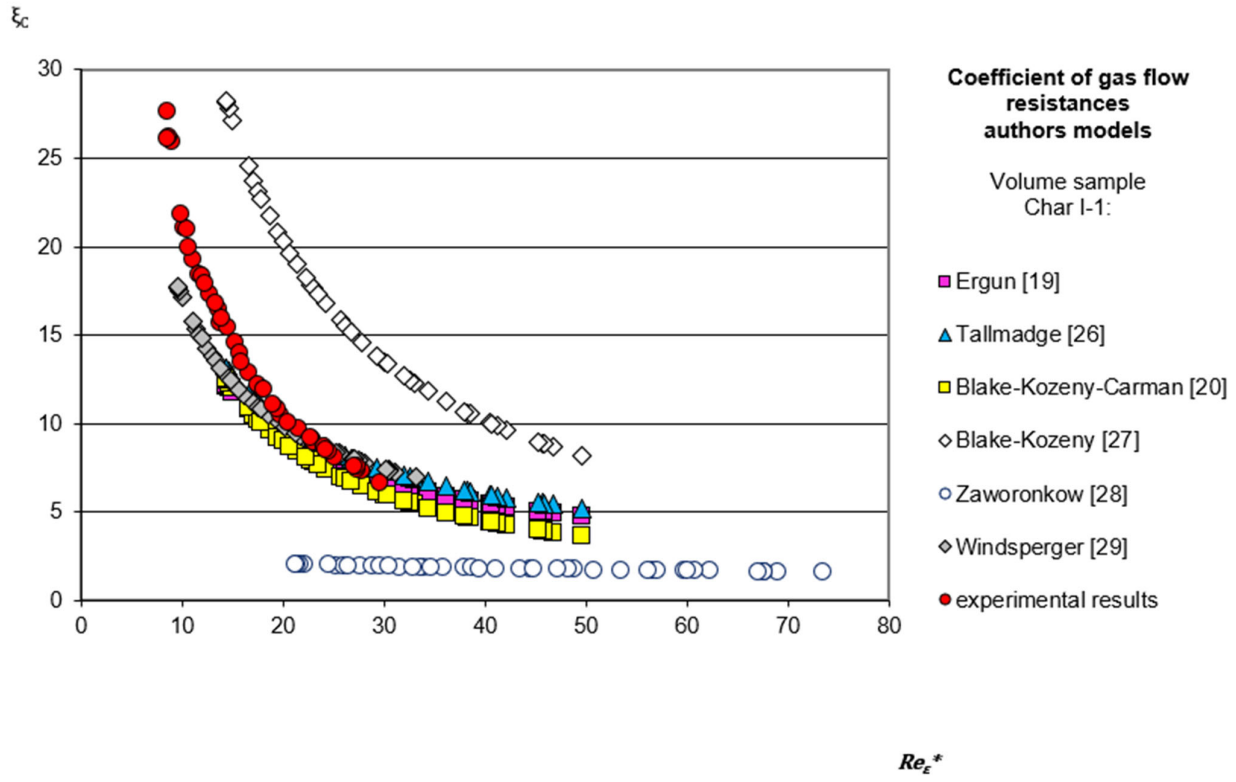

Figure 6. Coefficient of resistances of gas flow through coal char according to authors' models [own elaboration].

The distribution of experimental points proves that except for the Zaworonkow [28] model and the Blake-Kozeny [27] model, all the remaining ones show the same trend of changes to this coefficient, which confirms the adequacy of the adopted assumptions.

In this research, direct measurements were taken and for this purpose instruments for measuring gas flow, pressure (pressure difference), and temperature were used. These instruments were properly calibrated, which resulted in the relation to the gas flow meters used which are given in Table 4.

Table 4. Parameters of gas flow meters calibration [own elaboration].

Flow Meter Type	Measurement Range	Scaling Equation—The Value of the Air Stream, dm³/min	Accuracy of Scaling
RDN 06-03	0 - 1.9	Q_g = (0.0137 scala) − 0.30086	0.97
R 10a	0 - 38	Q_g = (0.2836 scala) + 9.9091	0.99
RDN 06-03	0 - 48	Q_g = (0.216·scala) + 1.4112	0.99
R 10m	0 - 51	Q_g = (0.4264 scala) + 9.5	0.99
R	0 - 1.5	Q_g = (10 mL/ measurement time)	±5%

The analysis of measurement error was also the subject of our consideration. It was found that with respect to the measured values, this analysis did not bring any significant improvement to the estimation of the measurement error. In this regard, the detailed description of the measurement error analysis was omitted.

By way of an example, the algorithm for calculating the error and the uncertainty of air volume flow measurement, which results from the analysis of measurement errors, is presented. The calculation results according to the algorithm are presented in Table 5.

Table 5. An algorithm concerning the analysis of measurement error [own elaboration].

Algorithm	Score
Expected value as an arithmetic mean.	3.74×10^{-4}
The measure of scattering, as a variance of the arithmetic mean.	1.07×10^{-10}
Standard deviation.	1.03×10^{-5}
The component of the measurement error limit: - a systematic border error, where the absolute error of the measuring instrument (RDN06-03 rotameter) is 5%.	1.87×10^{-6}
The component of the measurement error limit: - accidental random error.	3.01×10^{-5}
Limit measurement error at the confidence level probability p~0.99.	3.29×10^{-5}
The result of the measurement at the confidence level p~0.99	$3.74 \times 10^{-4} \pm 3.29 \times 10^{-5}$

As can be seen from Table 5, expected (average) value for the adopted measurement is 3.74×10^{-4} m^3/s, at the result (at the confidence level 0.99) $3.74 \times 10^{-4} \pm 3.29 \times 10^{-5}$ m^3/s, which gives an average measurement error for the analyzed series of 8.7%. The average relative mistake for the entire scope of the flow of gas amounted to ± 5.3%.

4. Conclusions

Hydrodynamic investigations were carried out which concerned gas bubbling conditions through char deposit. This made it possible to assess such hydrodynamic parameters such as the permeability of the porous material and the resulting flow resistance coefficient. The assessment of hydrodynamic parameters related to gas permeability showed that the remaining models available in the literature show the correct correlation with the obtained test results. This situation should be explained by the limited scope of applying these models to skeletal centers characterized by a significant internal structure of the porous material.

This study's model of the identification of the permeability coefficient of porous materials, based on achieved results, was based on the value of the local opposition of the flow which correctly reflected tendencies of changes of hydrodynamic parameters.

The results of this research indicate that in the bubbling conditions it is possible to accurately assess these parameters, which gives the opportunity to comprehensively evaluate the properties of the porous material in the process aspect for gas production technology.

Based on research conducted so far, it can be stated that when gas flows through porous media with channel dimensions—of the order of millimeters and

less—hydrodynamic phenomena (gas flow, viscosity) are dominant over physicochemical phenomena (shaping the structure and mechanical properties) occurring at the interface; the latter, however, are important in flows through structures with very small pore sizes—on the order of a few tenths of a micrometer.

Given the above, it seems that a broader knowledge and description of the hydrodynamics of gas flow through porous materials and the connection of this phenomenon with the internal structure of the tested material is expedient in both cognitive and application terms. Having a universal method of determining permeability, both in laboratory tests and as part of the interpretation of technological processes, can be used to improve process efficiency, for example.:

(a) fermentation of the substrate on porous beds using immobilization as a result, striving to obtain over 90% of methane in raw biogas.
(b) extraction of methane from coal seams, both in pre-methane drainage as well as methane drainage carried out during and after operation.
(c) in situ gasification of coal, in which the deposit is converted at the site of its deposition and its effect is the production of raw gas with high energy parameters.

Funding: The study was carried out in the framework of: (1) the project under the program BIOSTRATEG founded by the National Centre for Research and Development "BIOSTRATEG1/269056/5/NCBR/2015 11 August 2015. (2) The Research Task (statutory) No. 11/79/2019 "Developing a model describing the gas permeability of anisotropic porous materials in the aspect of adhesive hydrodynamics for agroenergetic applications" implemented by the Renewable Energy Department in the Poznan Branch, Institute of Technology and Life Sciences in Falenty. The APC was funded by Institute of Technology and Life Sciences in Falenty.

Institutional Review Board Statement: Not applicable.

Informed Consent Statement: Not applicable.

Data Availability Statement: The data presented in this study are available on request from the corresponding author.

Conflicts of Interest: The authors declare no conflict of interest. The funders had no role in the design of the study; in the collection, analyses, or interpretation of data; in the writing of the manuscript; or in the decision to publish the results.

Abbreviations

Main symbols

A	total cross-section of the flow channel	m^2
K	permeability coefficient	m^2
L	flow path length for the height of the porous bed	m
P	pressure gauge	Pa
Q	volumetric flow	m^3/s
Re	Reynolds number	
T	thermometer	°C
V	volume	m^3
a	experimental constant	
e	indicator porosity	
d	diameterm	
f	function	
w	velocitym/s	
ΔP	pressure drop, resistance flow	Pa
Ψ	tortuosity	
ε	porosity	
η	fluid viscosity	Pa·s
λ	coefficient of linear resistance	
ξ	coefficient of flow resistance	

π	Pi number	
ρ	fluid density	kg/m^3
χ	coefficient of tortuosity	
ϑ	density of a solid body	kg/m^3
Upper indices refer to		
*	own model	
n	constant	
Lower indices refer to		
B	acc. Brauer	
B-K	acc. Blake-Kozeny	
B-K-C	acc. Blake-Kozeny-Carman	
B-P	acc. Burke-Plummer	
E	acc. Ergun	
T	acc. Tallmadge	
W	acc. Windsperger	
Z	acc. Zaworonkow	
a	apparent	
b	absolute	
c	total	
e	equivalent	
ef	effective	
g	gas	
o	value calculated on the total deposit section—apparent value	
r	nozzle	
re	reference	
s	skeleton	
zm	measured	
ε	value calculated relative to the porosity	

References

1. Dyrka, I. *Cechy Petrofizyczne Skał Łupkowych. Państwowa Służba Geologiczna o Gazie w Łupkach. Środowisko Występowania łupków Gazonośnych [Petrophysical Features of Shale Rocks. The National Geological Survey on Shale Gas. The Environment of Occurrence of Gas-Bearing Shales]*; Państwowy Instytut Geologiczny—Państwowy Instytut Badawczy: Warszawa, Poland, 2013; Volume 3, pp. 44–47.
2. Caillet, G.; Judge, N.C.; Bramwell, N.P.; Meclani, L.; Green, M.; Ada, P. Overpressure and hydrocarbon trapping in the Chalk of the Norwegian Central Graben. *Pet. Geosci.* **1997**, *3*, 33–42.
3. Carter, K.M.; Harper, J.A.; Schmid, K.W.; Kostelnik, J. Unconventional natural gas resources in Pennsylvania: The backstory of the modern Marcellus Shale play. *Environ. Geosci.* **2011**, *18*, 217–257, doi:10.1306/eg.09281111008.
4. Dasgupta, S.; Chayyerjee, R.; Mohanty, S.P. Magnitude, mechanisms and prediction of abnormal pore pressure using well data in the Krishna Godavari Basin, East coast of India. *AAPG Bull.* **2016**, *100*, 1833–1855.
5. Dixit, N.C.; Hanks, C.L.; Wallace, W.K.; Ahmadi, M.; Awoleke, O. In Situ Stress Variations Associated with Regional Changes in Tectonic Setting, northeastern Brooks Range and eastern North Slope of Alaska. *AAPG Bull.* **2017**, *48*, 10107–10115.
6. Fan, C.Y.; Wang, Z.L.; Wang, A.G.; Fu, S.T.; Wang, L.Q.; Zhang, Y.S.; Kong, H.X.; Zhang, X. Identification and calculation of transfer overpressure in the northern Qaidam Basin, Northwest China. *AAPG Bull.* **2016**, *100*, 23–39.
7. Hill, D.G.; Nelson, C.R. *Gas Productive Fractured Shales: An Overview and Update, Gas TIPS*; Gas Research Institute: Chicago, IL, USA, 2000; Volume 6, pp 4–18.
8. Lampe, C.; Song, G.Q.; Cong, L.Z.; Mu, X. Fault control on hydrocarbon migration and accumulation in the Tertiary Dongying depression, Bohai Basin, China. *AAPG Bull.* **2012**, *96*, 983–1000.
9. Lee, M.K.; Williams, D.D. Paleohydrology of the Delaware Basin, Western Texas: Overpressure Development, Hydrocarbon Migration, and Ore Genesis. *AAPG Bull.* **2000**, *84*, 171–180.
10. Liu, Y.F.; Qiu, N.S.; Xie, Z.Y.; Yao, Q.Y.; Zhu, C.Q. Overpressure compartments in the Central Paleo-Uplift, Sichuan Basin, southwest China. *J. Nat. Gas Sci. Eng.* **2016**, *100*, 867–888.
11. Osborne, M.J.; Swarbrick, R.E. Mechanisms for generating overpressure in sedimentary basins: A reevaluation. *AAPG Bull.* **1997**, *81*, 1023–1041.
12. Tingay, M.R.P.; Hillis, R.R.; Swarbrick, R.E.; Morley, C.K.; Damit, A.R. Origin of overpressure and pore-pressure prediction in the Baram province, Brunei. *AAPG Bull.* **2009**, *93*, 51–74.

13. Wu, J.; Liu, S.G.; Wang, G.Z.; Zhao, Y.H.; Sun, W.; Song, J.M.; Tan, Y.Y. Multi-Stage Hydrocarbon Accumulation and Formation Pressure Evolution in Sinian Dengying FormationCambrian Longwangmiao Formation, Gaoshiti-Moxi Structure, Sichuan Basin. *J. Earth Sci.* **2016**, *27*, 835–845.
14. Xu, Q.; Shi, W.; Xie, Y.; Wang, Z.; Li, X.; Tong, C. Identification of low-overpressure intervaland its implication to hydrocarbon migration: Casestudy in the Yanan sag of the Qiongdongnan Basin, South China Sea. *PLoS ONE* **2017**, 12, e0183676, doi:10.1371/journal.pone.0183676Editor.
15. Zeng, L, Microfracturing in the Upper Triassic Sichuan Basin Tight-gas Sandstones: Tectonic, Overpressure, and Diagenetic origins. *AAPG Bull.* **2010**, *94*, 1811–1825.
16. Amao, A.M. Mathematical Model for Darcy Forchheimer Flow with Applications to Well Performance Analysis. Master's Thesis, Department of Petroleum Engineering, Texas Tech University: Lubbock, TX, USA, 2007.
17. Bębenek, B.; Bębenek, H. *Straty Energii w Przepływach Płynów [Energy Losses in Fluid Flows]*; Wydawnictwo Politechniki Krakowskiej: Cracow, Poland, 1987.
18. Błaszczyk, M. Badanie Procesów Migracji Substancji Ropopochodnych i ich Emulsji w Strukturach Porowatych. Praca Dokotorska [Research upon Processes of Migration of Petroleum Substances and Their Emulsions in Porous Structures]. Doctoral Thesis, Politechnika Łódzka, Wydział Chemiczny, Łódź, Poland, 2014.
19. Ergun, S. Fluid flow through packed columns. *Chem. Eng. Prog.* **1952**, 48, 89–94.
20. Kembłowski, Z.; Michałowski, S.; Strumiłło, C.; Zarzycki, R. *Podstawy Teoretyczne Inżynierii Chemicznej i Procesowej [Theoretical Foundations of Chemical and Process Engineering]*; WN-T: Warsaw, Poland, 1985.
21. Orzechowski, Z.; Prywer, J.; Zarzycki, R. *Mechanika Płynów w Inżynierii i Ochronie Środowiska [Fluid Mechanics in Engineering and Environmental Protection]*; Wydawnictwo Naukowo-Techniczne, Warsaw, Poland, 2009.
22. Piecuch, T. Równanie Darcy jako podstawa analizy teoretycznej szczególnych przypadków procesu filtracji [Darcy equation as the basis for theoretical analysis of specific cases of the filtration process.]. *Rocz. Ochr. Środowiska* **2009**, *11, 299-319*.
23. Strzelecki, T.; Kostecki, S.; Żak, S. *Modelowanie Przepływów Przez Ośrodki Porowate [Flow Modeling through Porous Media]*; Dolnośląskie Wydawnictwo Edukacyjne: Wroclaw, Poland, 2008.
24. Peszyńska, M.; Trykozko, A.; Sobieski, W. Forchheimer law in the computational and experimental of flow through porous media at porescale and mesoscale. GAKUTO International Series. *Math. Sci. Appl.* **2010**, *32*, 463–482.
25. Brauer, H. *Grundlagen der Einphasen-und Mehrphasenströmungen*; Verlag Säuerländer: Frankfurt am Main, Germany, 1971.
26. Kasieczka, W. *Badanie Hydrodynamiki złoża Fluidalnego. Laboratorium. Kotły i Wytwornice Pary. Ćwiczenie nr K-07 [Investigation of Hydrodynamics of a Fluidized Bed. Lab. Boilers and Steam Generators. Exercise No. K-07]*; Katedra Techniki Cieplnej i Chłodnictwa, Politechnika Łódzka: Łódz, Poland, 2011; pp. 1–18.
27. Guimard, P.; McNerny, D.; Saw, E.; Yang, A. *Pressure Drop for Flow through Packed Beds*; Team 4; 06-363 Transport Process Laboratory; Carnegie Mellon University: Pittsburgh, PA, USA, 18 March 2004; pp. 1–14.
28. Zaworonkow, M.N. *Gidrawliczeskije Osnowy Skrubbernogo Processa i Tiepłopieredacza w Skrubberach*; Izd. Sow. Nauka: Mscow, Russia, 1944.
29. Windsperger, A. Abschätzung von spezifischer Oberfläche und Lückengrad bei biologischen Abluftreinigungsanlagen durch Vergleich von berechneten und experimentell erhaltenen Druckverlustwerten. *Chem. Ing. Tech.* **1991**, *63*, 80–81.
30. Di Sarlia, V.; Di Benedettob, A. Modeling and simulation of soot combustion dynamics in a catalytic diesel particulate filter. *Chem. Eng. Sci.* **2015**, 137, 69–78, doi:10.1016/j.ces.2015.06.011.
31. Cybulski, A.; Moulijn, J.A. Monoliths in heterogeneous catalysis. *J. Catal. Rev. Sci. Eng.* **1994**, *36*, 179.
32. Williams, J.L. Monolith structures, materials, properties and uses. *Catal. Today* **2001**, *69*, 3.
33. Wiatowski, M.; Stańczyk, K.; Świądrowski, J.; Kapusta, K.; Cybulski, K.; Krause, E.; Grabowski, J.; Rogut, J.; Howaniec, N.; Smoliński, A. Semi-technical underground coal gasification (UCG) using the shaft method in Experimental Mine "Barbara". *Fuel* **2012**, *99*, 170–179.
34. Stańczyk, K.; Kapusta, K.; Wiatowski, M.; Świądrowski, J.; Smoliński, A.; Rogut, J.; Kotyrba, A. Experimental simulation of hard coal underground gasification for hydrogen production. *Fuel* **2012**, *91*, 40–50.
35. Peszyńska, M.; Trykozko, A.; Pore-to-Core simulations of flow with large velocities using continuum models and imaging data. *Comput. Geosci.* **2013**, *17*, 623–645, doi:10.1007/s10596-013-9344-4.
36. Bear, J.; Cheng, A. *Modeling Groundwater Flow and Contaminant Transport*; Springer: Berlin/Heidelberg, Germany, 2010.